J. Fluid Mech. (2019), *vol.* 872, *pp.* 348–366.
doi:10.1017/jfm.2019.402

Three-dimensional effects on the transfer function of a rectangular-section body in turbulent flow

Yang Yang[1], **Mingshui Li**[1,2,†] **and Haili Liao**[1,2]

[1]Research Centre for Wind Engineering, Southwest Jiaotong University, Chengdu 610031, China

[2]Key Laboratory for Wind Engineering of Sichuan Province, Chengdu 610031, China

(Received 11 October 2018; revised 7 May 2019; accepted 7 May 2019;
first published online 10 June 2019)

This paper investigates the influence of three-dimensional effects on the transfer function of a rectangular-section body in turbulent flow. The dimensionless factor ψ, as derived by Li *et al.* (*J. Fluid Mech.*, vol. 847, 2018, pp. 768–785), is adapted to evaluate this influence. The calculation of ψ requires the spanwise influence term. For this purpose, an adapted form of the lift coherence function is derived, enabling the use of the measured lift coherence for the estimation of the spanwise influence term. Three rectangular models with different cross-sections (chord-to-depth ratios of 3, 5 and 10) are chosen for testing, and a NACA 0015 airfoil model is tested for comparison. Using the measured spanwise influence terms, the dimensionless factors of these models are then numerically calculated under different ratios of the turbulent integral scale to the chord γ and aspect ratios θ. It is shown that the dimensionless factors of the rectangular models increase as γ and θ increase, which are similar to the dimensionless factor of the airfoil model. If γ and θ have suitable values, the strip theory could be applicable to the rectangular-section body. It is also found that the dimensionless factors of all the rectangular models are larger than the dimensionless factor of the airfoil model under the same parameters. The smaller the chord-to-depth ratio is, the larger the dimensionless factor is. Using the strip theory to calculate the lift response of the rectangular-section body may provide more accurate estimation. Additionally, the one-wavenumber transfer functions of these models are determined under the consideration of the three-dimensional effects. The results show that the experimental transfer functions of the rectangular models cannot be captured by the Sears function. They are larger than the Sears function at lower frequencies, while falling at a faster rate as the frequency increases. For bluff bodies with separated flow, the modified transfer function presented here appears to be an appropriate approach.

Key words: aerodynamics, flow–structure interactions, turbulent flows

1. Introduction

The aerodynamic behaviour of a structure in unsteady flow has received considerable attention over several decades, and one of the important issues is the estimation of

†Email address for correspondence: lms_rcwe@126.com

the aerodynamic loading induced by turbulent flow. Liepmann (1952) first calculated the lift response of an ideal flat plate in turbulent flow under two assumptions. One was that the turbulent flow was fully correlated in the spanwise direction. The other was that each chordwise strip was two-dimensional and the transfer function was only a function of the chordwise wavenumber. The second assumption is generally called the strip theory. In reality, since the turbulent flow is three-dimensional, a consideration of the spatial variation of the turbulent flow would be closer to the physical nature of the problem. Hakkinen & Richardson (1957) corrected the spanwise variation of the turbulent flow, then calculated the lift on an airfoil in turbulent flow based on the strip theory. However, they found that the measured lift was still inconsistent with the theoretical estimation. The underlying cause for this discrepancy is the influence of three-dimensional effects on the transfer function. According to the three-dimensional theory, the kinematical boundary condition contains the chordwise and spanwise wavenumbers due to the chordwise and spanwise variations of the turbulent flow, leading to the transfer function being a function of chordwise and spanwise wavenumbers. Graham (1970, 1971) proposed a numerical method to calculate the exact value of the two-wavenumber transfer function of an ideal flat plate. Later, closed-form approximations for the two-wavenumber transfer function were derived by Mugridge (1971) and Blake (1986).

Though the three-dimensional theory can provide an accurate estimation of the lift force (Jackson, Graham & Maull 1973; McKeough 1976; Li, Li & Liao 2015), the much simpler strip theory is still of interest in practical applications because its use can simplify the related calculations. From an experimental point of view, the one-wavenumber transfer function is also much easier to determine. The accuracy of the strip theory is closely related to the degree of the influence of three-dimensional effects on the transfer function. In many previous experiments concerning airfoils and other streamlined structures (Jackson *et al.* 1973; Larose & Mann 1998; Larose 1999; Ma 2007), it was found that the influence of three-dimensional effects decreases as the ratio of the turbulence integral scale to the chord increases. However, it is usually difficult to achieve a large enough turbulence integral scale to chord ratio to render the influence of the three-dimensional effects negligible, which limits the application of the strip theory. Following the line of thought presented by Massaro & Graham (2015), Li *et al.* (2018) recently experimentally investigated the lift of a finite specified spanwise length of a two-dimensional airfoil in grid turbulence. The work confirmed that the influence of three-dimensional effects on the transfer function of an airfoil in turbulent flow depends not only on the ratio of the turbulence integral scale to the chord but also on the aspect ratio. This expands the conditions for the strip theory to apply.

In this study, we extend the previous work for application to a bluff body of rectangular cross-section because many structures encountered in nature and engineering situations are bluff bodies. As a typical bluff body, the rectangular-section body is one of the simplest shapes, yet has all the salient aerodynamic features of bluff bodies. A key quantity that needs to be known in this work is the spanwise influence term. However, unlike that of the airfoil, the spanwise influence term of the rectangular-section body cannot be obtained by theoretical derivation since the flow over the rectangular cross-section is partially separated, which inhibits the use of the theoretical model introduced by the previous work. In contrast to the previous work, an adapted form of the lift coherence function is derived in the present work and an empirical model for the spanwise influence term is given, enabling the use of the measured lift coherence for the estimation of the spanwise influence term.

With the measured spanwise influence term, the influence of three-dimensional effects on the transfer function and the applicability of the strip theory in the lift estimation of rectangular-section bodies can be analysed. In addition, the Sears function which is derived from the thin airfoil theory (Sears 1938) is a common one-wavenumber transfer function used in the engineering community. However, for bluff bodies, such as the rectangular-section body studied in this work, the Sears function may not be applicable due to the separated flow nature of the bluff body. In this case, the measurement of the one-wavenumber transfer function becomes necessary. Here, we introduce an approach to determining the one-wavenumber transfer function of a body in turbulent flow including the consideration of three-dimensional effects. Based on this approach, the one-wavenumber transfer functions of rectangular-section bodies are determined, which may provide a useful reference for bluff bodies with separated flow.

2. Theoretical description

In § 2.1, the unsteady lift response of a rectangular-section body to the turbulent flow is described. In § 2.2, the influence of three-dimensional effects on the lift is reflected by the three-dimensional (3-D) effects factor, and a dimensionless factor is introduced to evaluate the influence of three-dimensional effects on the transfer function. In § 2.3, an adapted form of the lift coherence function is derived with the aim of using the measured lift coherence to estimate the spanwise influence term. Note that the rectangular-section body studied here is a rectangular planform element of effectively infinite span with a constant rectangular cross-section, so the tip effect is not considered.

2.1. *Unsteady lift response of a rectangular-section body in turbulent flow*

The turbulent flow is three-dimensional. The phase of the fluctuating velocity varies not only in the chordwise direction but also in the spanwise direction. The Fourier component of the fluctuating velocity of the turbulent flow can therefore be expressed as an oblique harmonic gust convected with the velocity U, which has the form $w = w_0 \mathrm{e}^{-\mathrm{i}(\omega t - k_1 x - k_2 y)}$, where w_0 is the gust amplitude, ω is the circular frequency, k_1 and k_2 are chordwise and spanwise wavenumbers, respectively. Let L be the lift per unit span of a section of spanwise length b, e.g. the finite span section shown in figure 1(*a*). According to the three-dimensional theory, the lift L acting on such a section (centred on y) of an infinite rectangular-section body subjected to an oblique harmonic gust can be expressed as

$$\begin{aligned} L &= \frac{1}{b}\int_{y-b/2}^{y+b/2} \underbrace{\hat{C}_s w_0 \mathrm{e}^{-\mathrm{i}(\omega t - k_2 y)}}_{\textit{quasi-steady}} \chi(\tilde{k}_1, \tilde{k}_2)\,\mathrm{d}y \\ &= \hat{C}_s \sin c(k_2 b/2) w_0 \mathrm{e}^{-\mathrm{i}\omega t} \chi(\tilde{k}_1, \tilde{k}_2), \end{aligned} \tag{2.1}$$

where $\hat{C}_s$ is the static force term. For rectangular-section bodies, the static force term is equal to $\rho U c(C_L' + C_D)/2$, where ρ is the fluid density, c is the chord length, C_L' is the slope of the lift coefficient curve and C_D is the drag coefficient. Also, $\sin c(k_2 b/2)$ is the sinc function, $\chi(\tilde{k}_1, \tilde{k}_2)$ is the two-wavenumber transfer function, $\tilde{k}_1$ $(=k_1 c/2)$ and $\tilde{k}_2$ $(=k_2 c/2)$ are the dimensionless chordwise and spanwise wavenumbers, respectively. The lift induced by turbulent flow may be composed of

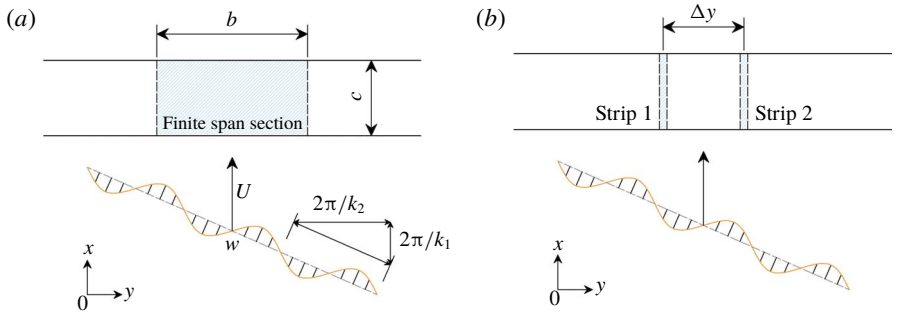

FIGURE 1. (Colour online) Sketch of an infinite rectangular-section body in turbulent flow, in which the Fourier component of the fluctuating velocity is represented by an oblique harmonic gust: (*a*) a finite span section with a spanwise length, (*b*) two strips separated in the spanwise direction.

the lift forces generated by a sum of such harmonic gust components (Ribner 1956; Etkin 1959). The two-dimensional spectrum of L is therefore written as

$$S_L(k_1, k_2) = \hat{C}_s^2 \sin c^2(k_2 b/2) S_w(k_1, k_2) |\chi(\tilde{k}_1, \tilde{k}_2)|^2, \tag{2.2}$$

where $S_w(k_1, k_2)$ is the two-dimensional vertical turbulence spectrum and $|\cdot|^2$ is the symbol for the squared modulus. Note that in cases where it does not result in confusion, the squared modulus of the transfer function is also referred to as the transfer function for the sake of brevity. The two-wavenumber transfer function can be expressed as the product of the one-wavenumber transfer function and the spanwise influence term (Mugridge 1971; Blake 1986), which is

$$|\chi(\tilde{k}_1, \tilde{k}_2)|^2 = |\chi(\tilde{k}_1)|^2 \eta(\tilde{k}_1, \tilde{k}_2), \tag{2.3}$$

where $\chi(\tilde{k}_1)$ is the one-wavenumber transfer function and $\eta(\tilde{k}_1, \tilde{k}_2)$ is the spanwise influence term. By integrating out the spanwise wavenumber, the one-dimensional lift spectrum can then be written as

$$S_L(k_1) = \hat{C}_s^2 |\chi(\tilde{k}_1)|^2 \int_{-\infty}^{+\infty} \sin c^2(k_2 b/2) S_w(k_1, k_2) \eta(\tilde{k}_1, \tilde{k}_2)\, \mathrm{d}k_2. \tag{2.4}$$

2.2. *Influence of three-dimensional effects on lift force and transfer function*

In order to bring in the one-dimensional vertical turbulence spectrum $S_w(k_1)$, the following 3-D effects factor is defined:

$$F_{3D}(k_1) = \frac{\displaystyle\int_{-\infty}^{+\infty} \sin c^2(k_2 b/2) S_w(k_1, k_2) \eta(\tilde{k}_1, \tilde{k}_2)\, \mathrm{d}k_2}{\displaystyle\int_{-\infty}^{+\infty} S_w(k_1, k_2)\, \mathrm{d}k_2}. \tag{2.5}$$

If the turbulence is homogeneous and isotropic, the turbulence spectrum can be described by the von Kármán spectral model (see appendix A). F_{3D} can then be

given in terms of dimensionless parameters: the ration of the vertical turbulence integral scale to the chord $\gamma = L_w^x/c$ and the ratio of the spanwise length to the chord (the aspect ratio) $\theta = b/c$,

$$F_{3D}(\tilde{k}_1, \gamma, \theta) = \frac{\int_{-\infty}^{+\infty} \sin c^2(\tilde{k}_2\theta)\xi_w(\tilde{k}_1, \tilde{k}_2, \gamma)\eta(\tilde{k}_1, \tilde{k}_2)\,\mathrm{d}\tilde{k}_2}{\int_{-\infty}^{+\infty} \xi_w(\tilde{k}_1, \tilde{k}_2, \gamma)\,\mathrm{d}\tilde{k}_2}, \tag{2.6a}$$

$$\xi(\tilde{k}_1, \tilde{k}_2, \gamma) = \frac{\tilde{k}_1^2 + \tilde{k}_2^2}{[1 + 28.688\gamma^2(\tilde{k}_1^2 + \tilde{k}_2^2)]^{7/3}}. \tag{2.6b}$$

The one-dimensional lift spectrum then becomes

$$S_L(k_1) = \hat{C}_s^2 S_w(k_1)|\chi(\tilde{k}_1)|^2 F_{3D}(\tilde{k}_1, \gamma, \theta). \tag{2.7}$$

From (2.7), the normalized one-dimensional lift spectrum $S_L/(\hat{C}_s^2 S_w)$ is the combination of the unsteady effects (reflected by the one-wavenumber transfer function) and the three-dimensional effects (reflected by the 3-D effects factor). This normalized one-dimensional lift spectrum can be directly obtained with the measured one-dimensional lift spectrum and the measured one-dimensional turbulence spectrum in practical measurements.

The 3-D effects factor includes the spanwise influence term due to the influence of three-dimensional effects on the transfer function. Following the work of Li *et al.* (2018), the dimensionless factor ψ, which is the ratio of the one-dimensional lift spectrum calculated from the three-dimensional theory and that calculated from the strip theory, can be used to evaluate the degree of this influence. According to the strip theory, the one-dimensional lift spectrum is

$$S_L(k_1) = \hat{C}_s^2 S_w(k_1)|\chi(\tilde{k}_1)|^2 F_{3DST}(\tilde{k}_1, \gamma, \theta), \tag{2.8}$$

where $F_{3DST}(\tilde{k}_1, \gamma, \theta)$ is the 3-D effects factor derived from the strip theory, in which the spanwise influence term is not included (or say, the spanwise influence term is equal to 1). It can be expressed as

$$F_{3DST}(\tilde{k}_1, \gamma, \theta) = \frac{\int_{-\infty}^{+\infty} \sin c^2(\tilde{k}_2\theta)\xi_w(\tilde{k}_1, \tilde{k}_2)\,\mathrm{d}\tilde{k}_2}{\int_{-\infty}^{+\infty} \xi_w(\tilde{k}_1, \tilde{k}_2)\,\mathrm{d}\tilde{k}_2}. \tag{2.9}$$

The dimensionless factor ψ is then expressed as

$$\psi(\tilde{k}_1, \gamma, \theta) = \frac{F_{3D}(\tilde{k}_1, \gamma, \theta)}{F_{3DST}(\tilde{k}_1, \gamma, \theta)} = \frac{\int_{-\infty}^{+\infty} \sin c^2(\tilde{k}_2\theta)\xi_w(\tilde{k}_1, \tilde{k}_2)\eta(\tilde{k}_1, \tilde{k}_2)\,\mathrm{d}\tilde{k}_2}{\int_{-\infty}^{+\infty} \sin c^2(\tilde{k}_2\theta)\xi_w(\tilde{k}_1, \tilde{k}_2)\,\mathrm{d}\tilde{k}_2}. \tag{2.10}$$

It can be seen that when the dimensionless factor is close to 1, F_{3D} can be approximated by F_{3DST}, which means that the influence of three-dimensional effects on the transfer function becomes negligible and the strip theory is applicable.

Actually, nothing has been gained so far because both the one-wavenumber transfer function and the spanwise influence term are unknown for the rectangular-section body. However, the lift coherence function is the ratio of the lift cross-spectrum to the lift auto-spectrum and consequently does not include the one-wavenumber transfer function. The possibility of using the measured lift coherence to determine the spanwise influence term becomes apparent.

2.3. *Coherence function of lift force*

The lift coherence is generally measured on two separate strips in the spanwise direction, e.g. strip 1 and strip 2 shown in figure 1(*b*). In this case, the lift of an infinitesimal span length $b \to 0$, and therefore the sinc function $\sin c(k_2 b/2) \to 1$. The lift coherence function is defined as

$$Coh_L(k_1, \Delta y) = \frac{S_L(k_1, \Delta y)}{S_L(k_1)}, \tag{2.11}$$

where Δy is the separation between two strips and $S_L(k_1, \Delta y)$ is the lift cross-spectrum, which can be expressed as the inverse Fourier transform of $S_L(k_1, k_2)$ as follows:

$$S_L(k_1, \Delta y) = \int_{-\infty}^{+\infty} S_L(k_1, k_2) \exp(\mathrm{i}k_2 \Delta y)\, \mathrm{d}k_2. \tag{2.12}$$

The lift coherence function is then written as

$$Coh_L(k_1, \Delta y) = \frac{\displaystyle\int_{-\infty}^{+\infty} S_w(k_1, k_2)\eta(\tilde{k}_1, \tilde{k}_2) \exp(\mathrm{i}k_2 \Delta y)\, \mathrm{d}k_2}{\displaystyle\int_{-\infty}^{+\infty} S_w(k_1, k_2)\eta(\tilde{k}_1, \tilde{k}_2)\, \mathrm{d}k_2}. \tag{2.13}$$

The spanwise influence term of the rectangular-section body cannot be theoretically derived since the flow over the rectangular cross-section is partially separated. However, a previous study (Li & Li 2017) indicated that an empirical solution may still be applicable in this case. For this, an empirical model of the spanwise influence term is given as follows:

$$\eta(\tilde{k}_1, \tilde{k}_2) = \frac{f(\tilde{k}_1)}{f(\tilde{k}_1) + \tilde{k}_2^2}, \tag{2.14a}$$

$$f(\tilde{k}_1) = a + \beta \tilde{k}_1^{\alpha}, \tag{2.14b}$$

where α, β and a are empirical parameters. In (2.13), a relation between the lift coherence and the spanwise influence term is established which enables the use of the measured lift coherence for the estimation of the empirical parameters in the spanwise influence term. Despite the empirical nature of this solution, it is believed that the fundamental properties of the results would not be lost. For comparison, the coherence function of the vertical fluctuating velocity is also given according to the preceding concepts as

$$Coh_w(k_1, \Delta y) = \frac{\displaystyle\int_{-\infty}^{+\infty} S_w(k_1, k_2) \exp(\mathrm{i}k_2 \Delta y)\, \mathrm{d}k_2}{\displaystyle\int_{-\infty}^{+\infty} S_w(k_1, k_2)\, \mathrm{d}k_2}. \tag{2.15}$$

Comparing (2.13) and (2.15), it can be seen that the lift coherence is naturally not equal to the coherence of the fluctuating velocity due to the influence of three-dimensional effects on the transfer function.

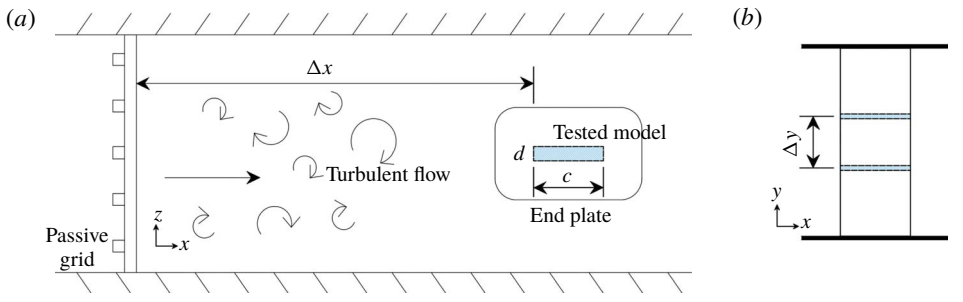

FIGURE 2. (Colour online) (*a*) Side view of the wind tunnel, the passive grid and the model. (*b*) Top view of the model.

3. Experimental set-up

The experiments are conducted in a closed-loop wind tunnel (XNJD-1) at Southwest Jiaotong University. The test section of the tunnel is 2.4 m wide and 2.0 m high. An overview of the experimental set-up is shown in figure 2(*a*). A square passive grid with a mesh size of 0.36 m and a bar width of 0.09 m is installed at the entrance of the test section to generate the turbulent flow. To ensure that the turbulent flow has enough time to develop to an approximately homogeneous and isotropic state, the distance from the measuring position to the grid is $\Delta x = 4.6$ m. The mean flow velocity is set to $U = 11.5$ m s^{-1}. To avoid the disturbance from the model, the characteristics of the flow field at the position of the leading edge of the model are measured in the empty wind tunnel, prior to the pressure measurement. Measurements are taken using the TFI Cobra Probe, which is a multi-hole pressure probe able to resolve three components of the flow velocity, with a frequency response of 0 Hz up to more than 2 kHz. The sampling frequency of the flow velocity measurement is 256 Hz, and the sampling time is 60 s. The dynamic frequency response of the Cobra Probe is stable during the measurement, ensuring the dynamic validity of the flow velocity data.

Three rectangular-cross-section models are tested and an airfoil model with a NACA 0015 profile is tested for comparison. The chord length of the airfoil model is $c =$ 0.4 m. The depths of all rectangular-cross-section models are $d = 0.06$ m, while the chord lengths are $c = 0.18$ m, 0.3 m and 0.6 m, respectively. The corresponding chord-to-depth ratios of these rectangular models are equal to 3, 5, 10, respectively. The models are made of ABS plastics, and several transverse glass fibre ribs are added to enhance their rigidity. During testing, the models are mounted horizontally (zero angle of attack) on the steel frame support. To simulate the infinite span conditions and prevent the air stream from flowing around the tips, end plates are installed at the sides of the model.

Surface pressures are measured using a Scanivalve ZOC33 miniature pressure scanner. Multiple pressure scanners are connected to the same Scanivalve DSM3400 digital service module, achieving synchronous acquisition of the pressures on different strips. The pressure scanners can sample pressure signals from 64 channels simultaneously, with an uncertainty of $\pm 0.08\%$ full scale. The pressure scanners are capable of reaching high dynamic response (in excess of 1 kHz). However, since the pressure signals are transmitted through the tubing connecting the taps to the pressure scanners, the dynamic response of the pressure measurement system also depends on the pneumatic frequency response of the tubing system. It is known that

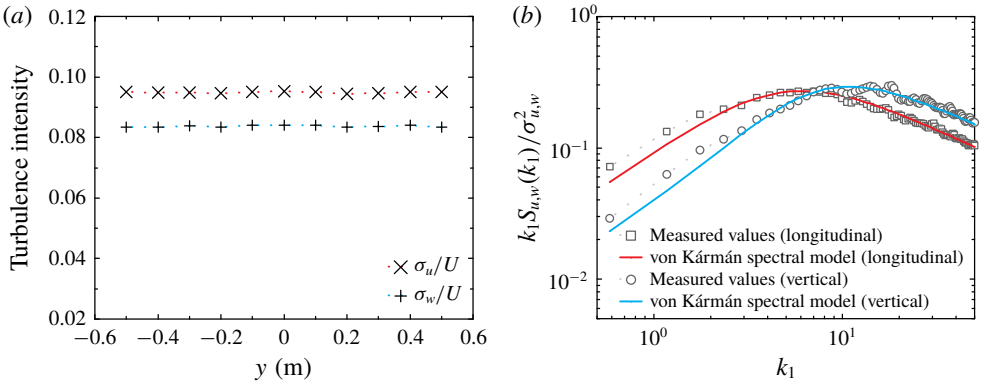

FIGURE 3. (Colour online) (*a*) Spanwise distributions of longitudinal and vertical normalized r.m.s. fluctuating velocities. (*b*) Comparisons between measured one-dimensional spectra of longitudinal and vertical fluctuating velocities and the von Kármán spectral models.

by the time the pressure signal reaches the scanner, it may potentially be skewed due to the resonance and damping effects developed in the tubing. Depending on the sampling frequency of the pressure, limiting the tubing length is a simple and effective approach to reducing the resonance and the damping effects to a point where they do not need to be considered (Ma 2007). In the current experiment, pressure scanners are placed directly inside the model to keep the tubing to less than 0.2 m. The sampling frequency of the pressure is 256 Hz and the duration of the measurement is 60 s. Within the length of 0.2 m, the resonance and damping effects in the tubing are small to negligible for the sampling frequency of 256 Hz, ensuring a good dynamic frequency response of the pressure measurement system during the measurement. The strips are located in the middle portion of the model. The separation between two strips is $\Delta y = 0.07$ m, as shown in figure 2(*b*). The lift of each strip and the lift coherence between two strips are then obtained using the measured pressures (see appendix B).

4. Results and discussion

4.1. *Characteristics of turbulent flow*

Grid turbulence is considered to be the closest practical approximation to homogeneous and isotropic turbulence. For homogeneous turbulence, the root mean square (r.m.s) of the fluctuating velocity should be identical everywhere in the same plane parallel to the grid. As shown in figure 3(*a*), the normalized r.m.s fluctuating velocities at different spanwise positions are very close. The homogeneity of the generated turbulence can be confirmed. The longitudinal and vertical normalized r.m.s fluctuating velocities are $\sigma_u/U = 0.095$ and $\sigma_w/U = 0.083$, respectively. The ratio $\sigma_u/\sigma_w = 1.14$. The turbulence integral scale, which reflects the mean size of the energy-containing eddies, can be determined by a comparison between the measured one-dimensional turbulence spectrum and the von Kármán spectral model (see appendix A). The measured one-dimensional spectra of the longitudinal and vertical fluctuating velocities are shown in figure 3(*b*). It can be seen that the measured turbulence spectra match well with the von Kármán spectral models, as observed in previous grid

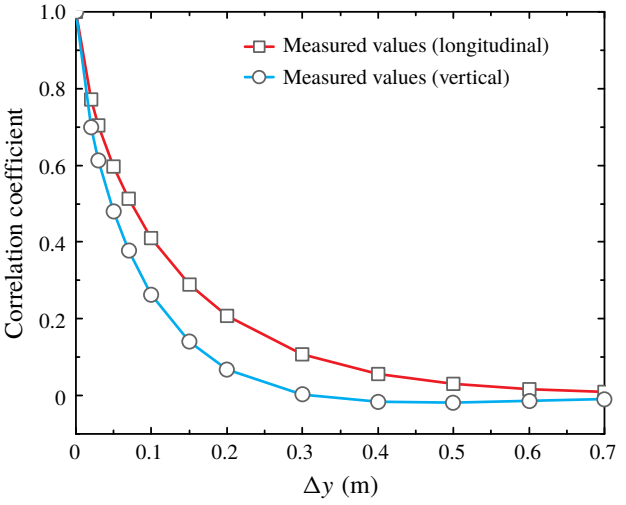

FIGURE 4. (Colour online) Spanwise correlation coefficients of longitudinal and vertical fluctuating velocities, Δy is the spanwise separation.

turbulence experiments (Roberts & Surry 1973; Nagata *et al.* 2011; Li *et al.* 2015). The longitudinal and vertical turbulence integral scales (in the chordwise direction) determined from the one-dimensional turbulence spectra are $L_u^x = 0.133$ m and $L_w^x = 0.062$ m, respectively. The ratio $L_u^x/L_w^x = 2.15$. To further assess the isotropy of the turbulence, the spanwise correlation coefficients of fluctuating velocities are measured, as shown in figure 4. The vertical turbulence integral scale in the spanwise direction can then be determined from the definition: $L_w^y = 0.06$ m and the ratio $L_u^x/L_w^y = 2.21$. Though it seems that the strictly isotropic condition is difficult to achieve, these results roughly satisfy the isotropic relationships and the generated turbulence can be regarded as approximately isotropic.

4.2. *Lift coherence and spanwise influence term*

The measured lift coherence and the measured coherence of the vertical fluctuating velocity are shown in figure 5. The theoretical velocity coherence is calculated by (2.15). Using (2.13) to fit the measured lift coherence, the empirical parameters of the spanwise influence term are obtained, as listed in table 1. The theoretical lift coherence of an ideal flat plate is also included for comparison. It is shown that the measured velocity coherence matches well with the theoretical velocity coherence, while the measured lift coherence is much stronger than the velocity coherence. This phenomenon has been shown experimentally on many occasions (Etkin 1971; Jakobsen 1997; Kimura *et al.* 1997; Larose & Mann 1998; Ma 2007). Etkin (1971) considered that the stronger correlation is an intrinsic property of the lift induced by the three-dimensional turbulence due to the influence of three-dimensional effects on the transfer function.

It can be observed that there are different degrees of deviation between the measured lift coherence of the model and the theoretical lift coherence of the ideal flat plate. Considering that the lift coherence reflects the structure of the flow around the body, the distortion of the velocity fluctuation and the flow separation may be the reasons for these deviations. Compared to the flow around an ideal flat plate,

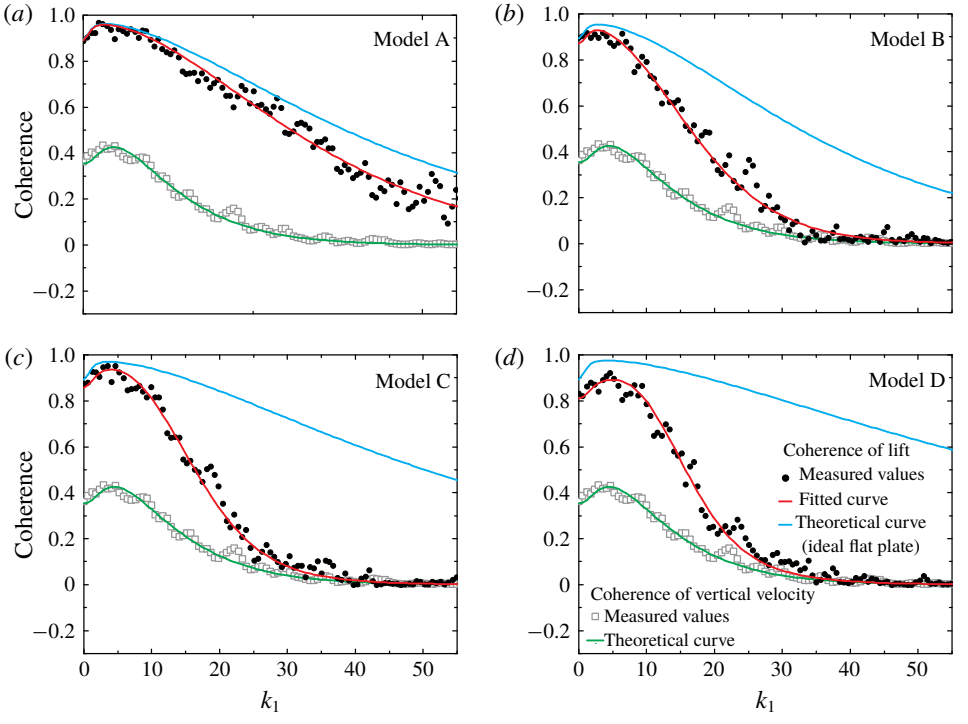

FIGURE 5. (Colour online) Coherence of lift forces and vertical fluctuating velocities.

	Configuration			Parameter		
	Cross-section	Chord	Depth	a	α	β
	Ideal flat plate			0.104	0.500	0.469
Model A	NACA 0015	0.40 m		0.156	1.101	0.653
Model B	Rectangular	0.60 m	0.06 m	0.306	1.795	1.400
Model C	Rectangular	0.30 m	0.06 m	0.467	2.393	3.266
Model D	Rectangular	0.18 m	0.06 m	0.653	2.632	5.250

TABLE 1. Parameters of spanwise influence term.

the mean velocity field of the flow around a real body is disturbed, which distorts the velocity fluctuation (or eddies) of the turbulent flow. The distortion of the velocity fluctuation reduces its spatial correlation (Santana *et al.* 2016) and consequently leads to the decrease of the coherence of the induced lift (compared to the theoretical lift coherence of the ideal flat plate). It should be noted that the deviation between the theoretical lift coherence and the measurement is frequency-dependent. As mentioned above, the turbulent flow is distorted by the disturbance of the mean velocity field; however, the degree of the distortion is different for eddies with different scales. The high-frequency velocity fluctuation (small-scale eddy) is more easily distorted by the disturbance than the low-frequency velocity fluctuation (large-scale eddy). Hence, the measured lift coherence agrees better with the theoretical value for lower frequencies, while for higher frequencies the measured lift coherence deviates significantly from the theoretical value due to the serious distortion of the velocity fluctuation. On the

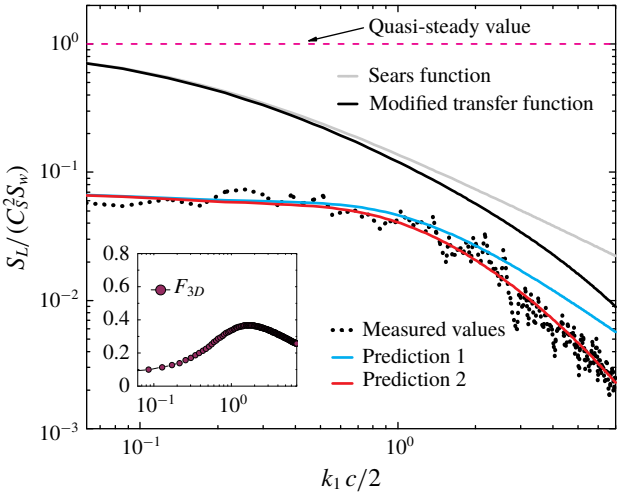

FIGURE 6. Normalized one-dimensional lift spectrum and transfer function of model A.

other hand, the flow over the rectangular cross-section is partially separated. The results indicate that the spatial correlation of the velocity fluctuation under separated flow conditions may be weaker than that under attached flow conditions, further reducing the lift coherence of the rectangular-section body compared to the lift coherence of the airfoil. It can be seen that the decrease of the lift coherence becomes more significant as the chord-to-depth ratio of the rectangular cross-section becomes smaller, accompanied by more serious flow separation.

It can be seen from these results that the turbulence distortion and flow separation have a significant influence on the lift coherence. Due to this influence, the lift coherence of a real body is lower than the theoretical lift coherence of an ideal flat plate, and the spanwise influence term of a real body is also different from the theoretical spanwise influence term. Compared to a rectangular-section body with larger chord-to-depth ratio, one with smaller chord-to-depth ratio experiences more serious turbulence distortion and flow separation. Correspondingly, the deviation between its lift coherence and the theoretical lift coherence is more obvious, and the difference between its spanwise influence term and the theoretical value is also more significant.

4.3. *Roles of 3-D effects factor and transfer function in lift force*

For a body in turbulent flow, factoring the lift only by the static force term would fail as the frequency increases since the generation of the lift is simultaneously affected by both the unsteady effects and the three-dimensional effects. As shown in figures 6–9, the one-dimensional lift spectrum, which is normalized by the one-dimensional turbulence spectrum and the static force term, decreases as the frequency increases. In this case, the 3-D effects factor F_{3D}, which is defined by (2.6*a*,*b*), can be used to reflect the influence of three-dimensional effects on the lift. Using the spanwise influence terms determined in § 4.2, the 3-D effects factors of the airfoil and rectangular-section bodies are calculated, as shown in the insets. The static force terms and ratios of turbulence integral scale to chord used in calculations are listed in table 2 in appendix C. Note that the aspect ratios are all equal to zero

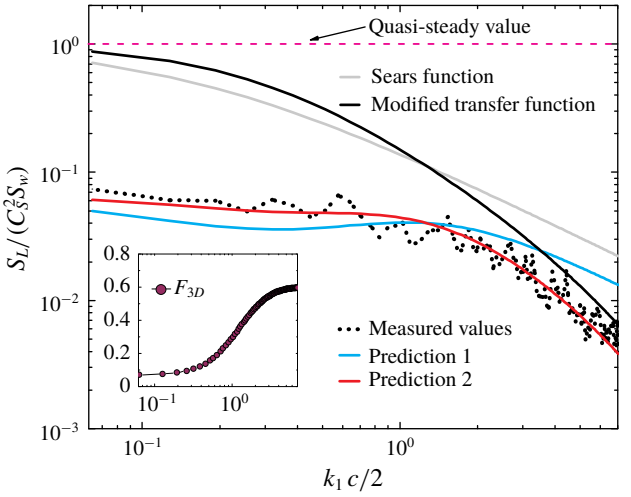

FIGURE 7. Normalized one-dimensional lift spectrum and transfer function of model B.

in the current experiment. The results show that the 3-D effects factor is a function with the value of less than 1, which is one of the reasons for the decreasing of the normalized lift spectrum compared to the quasi-steady value. The 3-D effect factor is relatively small at lower frequencies, but increases as the frequency increases. This indicates that the three-dimensional effects mainly affect the lift at lower frequencies, and the increase of the frequency tends to reduce this influence. In fact, we will show in the next section that the influence of three-dimensional effects on the lift reaches a peak at a certain frequency and then decreases as the frequency increases. Certainly, the 3-D effects factors of these aerodynamic configurations are different due to their different spanwise influence terms as well as the ratios turbulence integral scale to chord.

The flow being unsteady is another reason for the decreasing of the normalized lift spectrum compared to the quasi-steady value. These unsteady effects can be reflected by the one-wavenumber transfer function, which would apply unchanged to the spanwise correlated unsteady incident flow. After separating the influence of three-dimensional effects on the lift with the 3-D effects factor, the one-wavenumber transfer functions of these aerodynamic configurations can then be determined based on experiment data. Due to the empirical nature of the determination, an empirical model for the one-wavenumber transfer function is introduced (see appendix C). For the NACA 0015 airfoil, the one-wavenumber transfer function agrees well with the Sears function at lower frequencies, while falling at a faster rate as the frequency increases, as shown in figure 6. According to previous theoretical studies (Goldstein & Atassi 1976; Atassi 1984; Lysak, Capone & Jonson 2013), this may be caused by the thickness effects. The Sears function is derived based on the flat plate assumption. This may be a reasonable assumption at lower frequencies. However, at higher frequencies, the turbulence is significantly distorted by the disturbance of the mean velocity caused by the thickness. In this case, the flat plate assumption is invalid and leads to the overestimation of the transfer function. Relatively little research has investigated the one-wavenumber transfer function of the rectangular-section body. From the results of figures 7–9, the one-wavenumber transfer functions of the rectangular-section bodies are larger than the Sears function at lower frequencies,

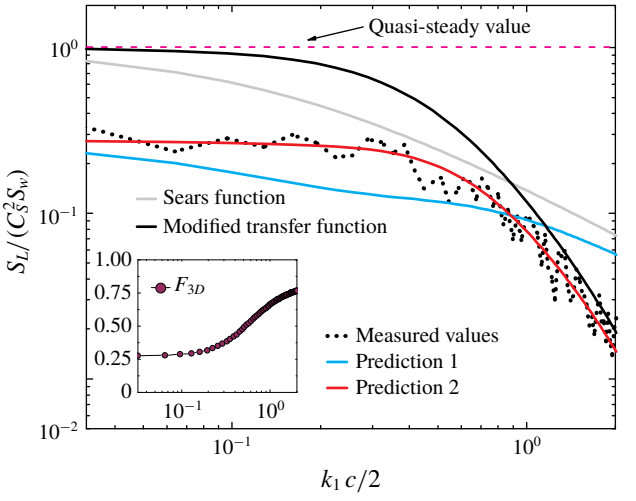

FIGURE 8. Normalized one-dimensional lift spectrum and transfer function of model C.

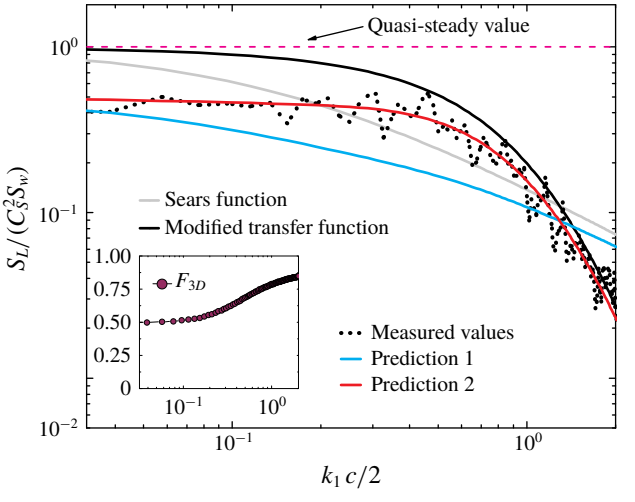

FIGURE 9. Normalized one-dimensional lift spectrum and transfer function of model D.

while also falling more quickly than the Sears function as the frequency increases. The high-frequency deviation may be attributed to the distortion of the turbulence, similarly to the case involving a thick airfoil. However, the physics that causes the low-frequency deviation is still not fully understood, to the extent that the role of the flow separation in the generation mechanism of the lift is not clear.

From the current results, it can be seen that the low-frequency deviation becomes more significant as the chord-to-depth ratio becomes smaller. This is accompanied by more serious flow separation. It may be considered that the flow separation reduces the influence of the unsteady effects on the lift at lower frequencies. The more serious the flow separation, the lower the influence of the unsteady effects on the low-frequency lift, and consequently the closer the one-wavenumber transfer function of the rectangular-section body to the quasi-steady value. To better illustrate these

differences, prediction 1 is calculated with the Sears function and the 3-D effects factor, while prediction 2 is calculated with the modified transfer function and the same 3-D effects factor. It can be seen that, although both predictions consider the three-dimensional effects, prediction 1 cannot capture the experimental values because the Sears function does not consider the effects of the flow separation and the distortion. Prediction 2, wherein the transfer function accounts for the effects of the flow separation and the distortion by modifying the Sears function, agrees well with experimental values. Hence, for rectangular-section bodies, the use of the Sears function would underestimate the lift at lower frequencies while overestimating the lift at higher frequencies. The modified transfer function proposed here may be an appropriate alternative in this case.

4.4. *Influence of turbulence integral scale to chord ratio and aspect ratio*

In § 4.3, we have shown that the three-dimensional effects have a significant influence on the lift induced by turbulent flow. This influence can be calculated by the 3-D effects factor F_{3D} derived from the three-dimensional theory. However, it requires the spanwise influence term to be known. If the strip theory is applicable, the simpler factor F_{3DST} derived from the strip theory can be used to approximate F_{3D}, avoiding the measurement of the spanwise influence term. The key is to what extent the strip theory is applicable. For this, F_{3D} and F_{3DST} are numerically calculated under different turbulence integral scale to chord ratios γ and aspect ratios θ, as shown in figure 10. The relative deviation between F_{3D} and F_{3DST} (the accuracy of the strip theory) is quantitatively evaluated by the dimensionless factor ψ under the same parameters, as shown in figure 11. Note that F_{3DST} does not contain the spanwise influence term, and is therefore independent of the aerodynamic configuration.

It is shown that the 3-D effects factors F_{3D} of all configurations are much smaller than F_{3DST} when the values of γ and θ are small. The use of the strip theory would thus lead to the significant overestimation of the lift in this case. As γ and θ increase, F_{3D} gradually approaches F_{3DST}. When the values of γ and θ are large, the deviation between F_{3D} and F_{3DST} becomes small. The same trend can be observed in the results of the dimensionless factor. The dimensionless factor ψ is much less than 1 when γ and θ have small values, and increases with the increase of γ and θ. When γ and θ have large values, the dimensionless factor ψ is close to 1. The deviation between F_{3D} and F_{3DST} (or say, the dimensionless factor ψ) also depends on the frequency. The deviation at lower frequencies is significantly larger than the deviation at higher frequencies, and therefore the dimensionless factor ψ is closer to 1 at higher frequencies. In addition, both F_{3D} and F_{3DST} reach a peak at a certain frequency then decrease as the frequency increases. The occurrence of the peak may be related to the shape of the turbulence spectrum. As is known, the turbulence spectrum also has a peak at the energy-containing range. From the correlation point of view, at the peak of the spectrum, the correlation of the turbulence is the strongest, and the three-dimensional effect is the weakest. F_{3D} and F_{3DST} reflect the influence of the 3-D effects on the lift, and therefore reach a peak at the frequency where the three-dimensional effect is the weakest. When the values of γ and θ are small, the peak position of F_{3D} is not identical with the peak position of F_{3DST} due to the influence of three-dimensional effects on the transfer function. With the increase of γ and θ, the influence of three-dimensional effects on the transfer function gradually weakens, and the positions of these peaks tend to be identical. It can be concluded from these results that for rectangular-section bodies, the accuracy of the strip theory

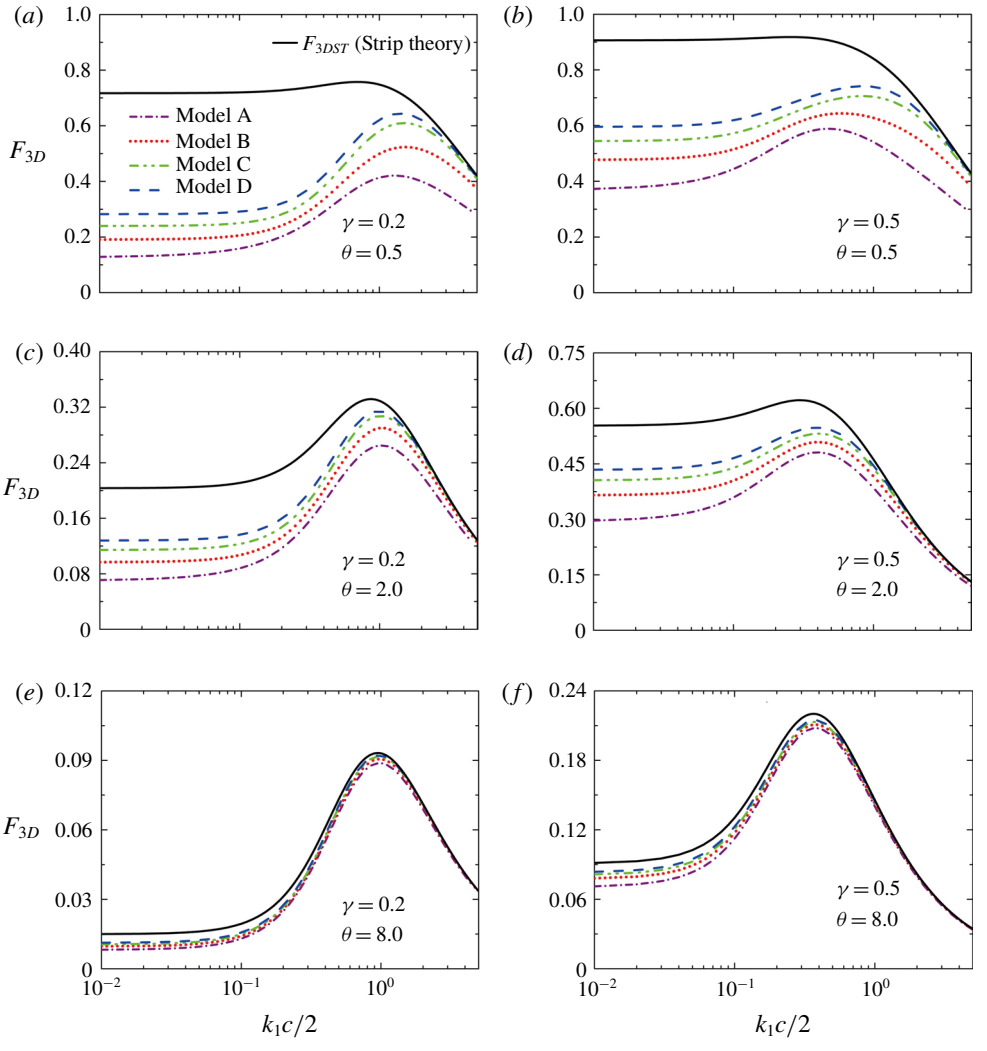

FIGURE 10. (Colour online) 3-D effects factors F_{3D} under different ratios of turbulence integral scale to chord γ and aspect ratios θ.

depends on the ratio of the turbulence integral scale to the chord as well as the aspect ratio, and is proportional to these two parameters. If these two parameters have suitable values, the strip theory can be applicable to the rectangular-section body, and F_{3DST} can be used to estimate the lift response of the rectangular-section body in turbulent flow.

The results also show that the dimensionless factors of the rectangular-section bodies are larger than the dimensionless factor of the airfoil under the same parameters. The dimensionless factor of the rectangular-section body with smaller chord-to-depth ratio is larger than that of the rectangular-section body with larger chord-to-depth ratio. As mentioned earlier, compared to the attached flow over the airfoil, the flow over the rectangular-section body is partially separated, and the flow separation experienced by the rectangular-section body with smaller chord-to-depth ratio is more serious. These trends imply that the accuracy of the strip theory is

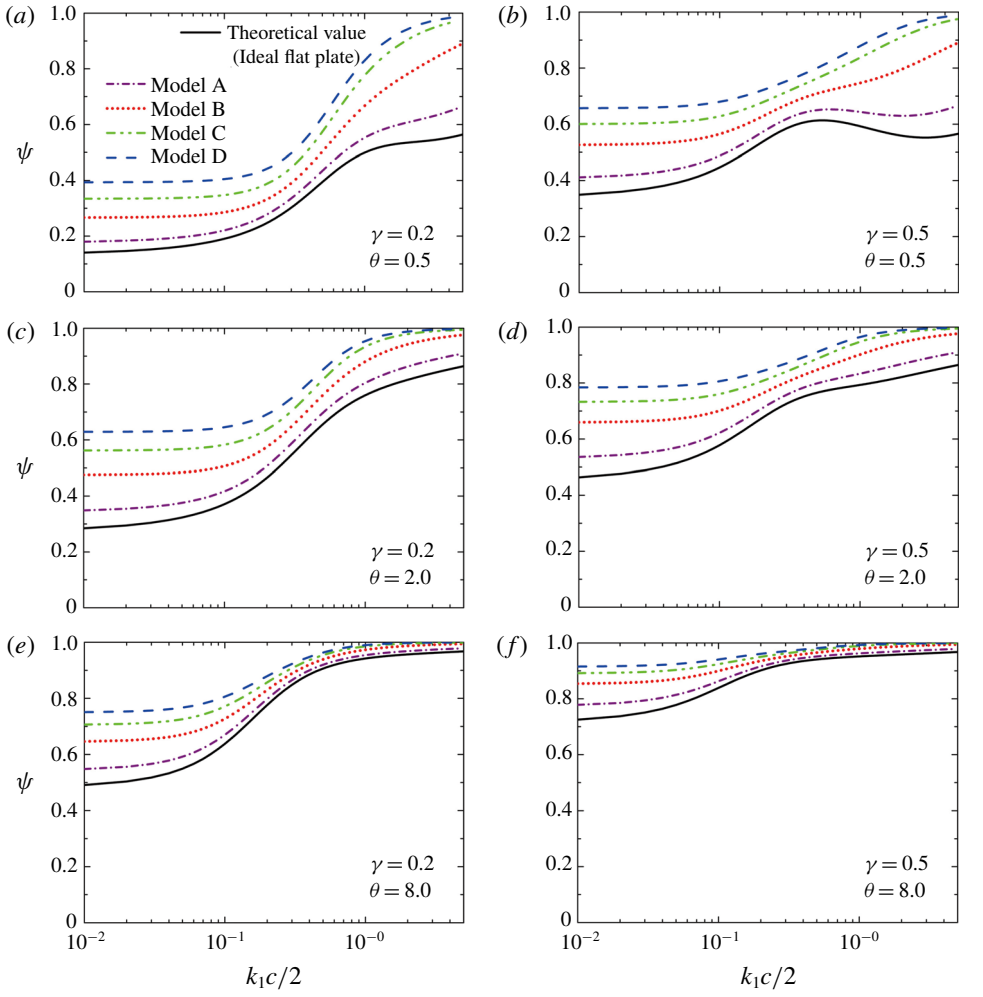

FIGURE 11. (Colour online) Dimensionless factors ψ under different of ratios turbulence integral scale to chord γ and aspect ratios θ.

improved under separated flow conditions. The flow separation is one of the salient aerodynamic features of bluff bodies. Hence, compared to the airfoil, the lift response of the bluff body calculated by the strip theory will have higher accuracy, and the more serious the flow separation, the higher the accuracy.

5. Conclusions

This study examines the influence of three-dimensional effects on the transfer function of a rectangular-section body in turbulent flow. A dimensionless factor which contains the spanwise influence term is introduced to evaluate this influence. For bluff bodies such as the rectangular-section body, the theoretical spanwise influence term is not applicable. An adapted form of the lift coherence function is thus derived and an empirical model for the spanwise influence term is given, enabling the use of the measured lift coherence for the estimation of the spanwise influence term.

The dimensionless factors of the rectangular-section bodies under different ratios of turbulent integral scale to chord and aspect ratios are then numerically calculated with the measured spanwise influence term. It is shown that the dimensionless factor of the rectangular-section body depends on both of the above ratios, and increases as they increase. This is in close agreement with findings regarding the airfoil in previous work. If the ratio of turbulent integral scale to chord and the aspect ratio have suitable values, the strip theory could also be applicable to the rectangular-section body. The results also reveal that the accuracy of the strip theory is improved under separated flow conditions. The more serious the flow separation, the higher the accuracy of the strip theory. Compared to the airfoil, the lift response of the rectangular-section body calculated by the strip theory may have higher accuracy. The flow separation is one of the salient aerodynamic features of bluff bodies. The current conclusions may also be applicable to other bluff bodies with separated flow, which would be helpful for simpler estimations of the lift responses of actual bluff structures.

In addition to the three-dimensional effects, the one-wavenumber transfer function of the rectangular-section body is also investigated. For this, an approach to determining the one-wavenumber transfer function of a body with consideration of three-dimensional effects is introduced. In this approach, the influence of three-dimensional effects on the lift is separated using the 3-D effects factor. The one-wavenumber transfer function is then obtained using the normalized lift spectrum and the 3-D effects factor. The results indicate that the one-wavenumber transfer function of the rectangular-section body is larger than the Sears function at lower frequencies, while falling at a faster rate as the frequency increases. This may be caused by the flow separation and the turbulence distortion. In terms of the trends of the results, the more serious the flow separation is, the closer the one-wavenumber transfer function is to the quasi-steady value. This implies that the flow separation reduces the influence of the unsteady effects on the lift. For bluff bodies, the use of the Sears function would underestimate the lift at lower frequencies and overestimate the lift at higher frequencies. The modified one-wavenumber transfer function proposed here, which takes the effects of the flow separation and distortion into account by modifying the Sears function, may be an appropriate alternative in this case.

Acknowledgements

This work was funded by the National Natural Science Foundation of China under grant nos 51478402, 51608074.

Appendix A. Spectral model for homogeneous isotropic turbulence

For homogeneous and isotropic turbulence, the spectrum can be described by the von Kármán model. The spectral models of the longitudinal fluctuating velocity are

$$S_u(k_1) = \frac{0.637\sigma_u^2 L_u^x}{[1 + 1.793(L_u^x)^2 k_1^2]^{5/6}}, \tag{A 1}$$

$$S_u(k_1, k_2) = \frac{0.38\sigma_u^2 (L_w^x)^2}{[1 + 1.793(L_u^x)^2 (k_1^2 + k_2^2)]^{4/3}}. \tag{A 2}$$

The spectral models of the vertical fluctuating velocity are

$$S_w(k_1) = \frac{0.637\sigma_w^2 L_w^x [1 + 19.125(L_w^x)^2 k_1^2]}{\left[1 + 7.172(L_w^x)^2 k_1^2\right]^{11/6}}, \tag{A 3}$$

$$S_w(k_1, k_2) = \frac{14.553\sigma_w^2 (L_w^x)^4 (k_1^2 + k_2^2)}{[1 + 7.172(L_w^x)^2 (k_1^2 + k_2^2)]^{7/3}}. \tag{A 4}$$

In the above equations, σ_u and σ_w are the r.m.s. longitudinal and vertical fluctuating velocities, respectively. L_w^x and L_w^x are the longitudinal and vertical turbulence integral scales, respectively.

Appendix B. Computation of lift force from pressure measurements

The lift on each strip can be obtained by integrating the measured pressure signals on the strip using the following formula:

$$L = \int_s (p_\infty - p) \sin\beta \, \mathrm{d}s \approx \sum_1^n (p_\infty - p_i) \sin\beta_i \Delta s_i, \tag{B 1}$$

where p_∞ is the reference pressure in the free stream, p_i is the pressure signal measured at the tap i on the model surface, Δs_i is the surface element length of the ith pressure tap and β_i is the angle between the normal direction of the surface element and the chord line. The lift coherence between two strips can be then calculated from the obtained lift on two strips using the following formula:

$$Coh = \frac{|S_{yy'}|}{\sqrt{S_y S_{y'}}}, \tag{B 2}$$

where $S_{yy'}$ is the cross-spectrum between two strips, S_y is the auto-spectrum on the y strip and $S_{y'}$ is the auto-spectrum on the y' strip.

Appendix C. Modified form of one-wavenumber transfer function

According to (2.7), the one-wavenumber transfer function can be expressed as

$$|\chi(\tilde{k}_1)|^2 = \frac{S_L(k_1)}{\hat{C}_s^2 S_w(k_1) F_{3D}(\tilde{k}_1, \gamma, \theta)}. \tag{C 1}$$

The 3-D effects factor $F_{3D}(\tilde{k}_1, \gamma, \theta)$ can be calculated by the use of (2.6*a*) and (2.6*b*). Using the measured one-dimensional lift spectrum and the measured one-dimensional vertical turbulence spectrum, the experimental values of the one-wavenumber transfer functions can then be determined. The parameters used in the calculation are listed in table 2. Here, with modification of the Sears function, the following modified form of the one-wavenumber transfer function is employed to fit the experimental data:

$$|\chi(\tilde{k}_1)|^2 = \frac{1}{1 + a_1 \tilde{k}_1^{a_2}} \exp(-\mu \tilde{k}_1), \tag{C 2}$$

where a_1, a_2, μ are empirical parameters which are determined by fitting the experimental values of the one-wavenumber transfer function, as listed in table 2.

	$\hat{C}_s$	γ	θ	a_1	a_2	μ
Model A	16.905	0.155	0	6.283	1.000	0.120
Model B	28.316	0.103	0	5.051	1.226	0.130
Model C	11.622	0.207	0	4.172	2.102	0.500
Model D	6.7190	0.344	0	1.260	2.211	0.980

TABLE 2. Parameters of modified one-wavenumber transfer function.

REFERENCES

ATASSI, H. M. 1984 The Sears problem for a lifting airfoil revisited—new results. *J. Fluid Mech.* **141**, 109–122.

BLAKE, W. K. 1986 *Mechanics of Flow-Induced Sound and Vibration*. Academic.

ETKIN, B. 1959 A theory of the response of airplanes to random atmospheric turbulence. *J. Aero. Sci.* **26**, 409–420.

ETKIN, B. 1971 *Dynamic of Atmospheric Flight*. Wiley.

GOLDSTEIN, M. E. & ATASSI, H. M. 1976 A complete second-order theory for the unsteady flow about an airfoil due to a periodic gust. *J. Fluid Mech.* **74**, 741–765.

GRAHAM, J. M. R. 1970 Lifting-surface theory for the problem of an arbitrary yawed sinusoidal gust incident on a thin aerofoil in incompressible flow. *Aeronaut. Q.* **21**, 182–198.

GRAHAM, J. M. R. 1971 A lift-surface theory for the rectangular wing in non-stationary flow. *Aeronaut. Q.* **22**, 83–100.

HAKKINEN, R. J. & RICHARDSON, A. S. 1957 Theoretical and experimental investigation of random gust loads. Part I. Aerodynamic transfer function of a simple wing configuration in incompressible flow. *NACA Tech. Rep.* 3878.

JACKSON, R., GRAHAM, J. M. R. & MAULL, D. J. 1973 The lift on a wing in a turbulent flow. *Aeronaut. Q.* **24**, 155–166.

JAKOBSEN, J. B. 1997 Span-wise structure of lift and overturning moment on a motionless bridge girder. *J. Wind Engng Ind. Aerodyn.* **69**, 795–805.

KIMURA, K., FUJINO, Y., NAKATO, S. & TAMURA, H. 1997 Characteristics of buffeting forces on flat cylinders. *J. Wind Engng Ind. Aerodyn.* **69**, 365–374.

LAROSE, G. L. 1999 Experimental determination of the aerodynamic admittance of a bridge deck segment. *J. Fluid Struct.* **13**, 1029–1040.

LAROSE, G. L. & MANN, J. 1998 Gust loading on streamlined bridge decks. *J. Fluid Struct.* **12**, 511–536.

LI, M., YANG, Y., LI, M. & LIAO, H. 2018 Direct measurement of the *S*ears function in turbulent flow. *J. Fluid Mech.* **847**, 768–785.

LI, S. & LI, M. 2017 Spectral analysis and coherence of aerodynamic lift on rectangular cylinders in turbulent flow. *J. Fluid Mech.* **830**, 408–438.

LI, S., LI, M. & LIAO, H. 2015 The lift on an aerofoil in grid-generated turbulence. *J. Fluid Mech.* **771**, 16–35.

LIEPMANN, H. W. 1952 On the application of statistical concepts to buffeting problem. *J. Aero. Sci.* **19**, 793–800.

LYSAK, P. D., CAPONE, D. E. & JONSON, M. L. 2013 Prediction of high frequency gust response with airfoil thickness effects. *J. Fluid Struct.* **39**, 258–274.

MA, C. 2007 3D Aerodynamic admittance research of streamlined box bridge decks. PhD thesis, Southwest Jiaotong University, Chengdu.

MASSARO, M. & GRAHAM, J. M. R. 2015 The effect of three-dimensionality on the aerodynamic admittance of thin sections in free stream turbulence. *J. Fluid Struct.* **57**, 81–89.

MCKEOUGH, P. 1976 Effects of turbulence on aerofoils at high incidence. PhD thesis, University of London.

MUGRIDGE, B. D. 1971 Gust loading on a thin aerofoil. *Aeronaut. Q.* **22**, 301–310.

NAGATA, K., HUNT, J. C. R., SAKAI, Y. & WONG, H. 2011 Distorted turbulence and secondary flow near right-angled plates. *J. Fluid Mech.* **668**, 446–479.

RIBNER, H. S. 1956 Spectral theory of buffeting and gust response: unification and extension. *J. Aero. Sci.* **23**, 1075–1077.

ROBERTS, J. B. & SURRY, D. 1973 Coherence of grid-generated turbulence. *J. Engng Mech. Div.* **99**, 1227–1245.

SANTANA, L. D., CHRISTOPHE, J., SCHRAM, C. & DESMET, W. 2016 A rapid distortion theory modified turbulence spectra for semi-analytical airfoil noise prediction. *J. Sound Vib.* **383**, 349–363.

SEARS, R. W. 1938 A systematic presentation of the theory of thin airfoils in non-uniform motion. PhD thesis, California Institute of Technology, Pasadena, CA.